

Received December 18, 2019, accepted January 19, 2020, date of publication January 29, 2020, date of current version February 6, 2020.

Digital Object Identifier 10.1109/ACCESS.2020.2970161

# Modeling and Visualization of Rice Roots Based on Morphological Parameters

LE YANG<sup>1,2</sup>, JUN PENG<sup>1</sup>, AND PENG SHAO<sup>1</sup>

<sup>1</sup>School of Computer and Information Engineering, Jiangxi Agricultural University, Nanchang 330045, China

<sup>2</sup>Agriculture Information Technology Key Laboratory of Universities in Jiangxi, Nanchang 330045, China

Corresponding author: Peng Shao (sp198310@163.com)

This work was supported by the National Natural Science Foundation of China (Name: Modeling and Visualization Simulation of Rice Root Based on Physiological Ecology, No. 61862032) and the Science and Technology Plan Projects of Jiangxi Provincial Education Department (Name: Design of digital filter based on PSO algorithm for processing of agricultural video images, No. GJJ160409).

**ABSTRACT** As an important organ of absorbing water and nutrients for rice, the cognition and expression of the three-dimensional (3D) morphology of roots has become a bottleneck in-depth study of rice roots due to the observing obstacles of soil. To clarify the morphological and distributional characteristics of rice roots, “root box” experiments are conducted to mensurate three dimensional spatial coordinates and morphological parameters of rice roots at different growth stages. Based on these experiments and the morphological parameters, the initial position of the root node and growth direction of branches are determined, a rice root model is constructed with B-spline curves by analyzing the topological structure of rice roots to quantify the biological characteristics of rice roots and summarize the morphological structure and growth characteristics of rice roots and improve the cubic growth function to describe the growth change in rice roots. Meanwhile, the output accuracy of the model is tested. In addition, dynamic simulation of rice root growth characteristics in 3D space is implemented using Visual C++ and the OpenGL standard graphics library. Analysis results indicate that the average simulated fitness of the total root length, surface area and volume is about 94.82%, 93.86%, and 91.96%, respectively. Therefore, the model can express the morphological characteristics and growth rules of rice roots at different growth stages, which enrich the digitization and visualization methods for roots of other crops.


**INDEX TERMS** B-spline curve, morphological parameters, rice roots, visualization.

## I. INTRODUCTION

As the “engine” of crop growth, the main function of roots is to absorb the moisture and nutrients needed for plant growth from the surrounding soil [19]. Morphological and physiological indices of crop roots are closely associated with the prophase stage of development of the aboveground parts of roots and with crop output and grain quality in the later stages. Therefore, root morphological and physiological characteristics must be optimized to guarantee good crop yields [37]. However, approximately 75% of rice crops are cultivated in soils under flood conditions during the growing season [2]; thus, the important parts of the plants are typically submerged making measurement and study difficult [12]. Moreover, crop roots do not exhibit the prominent growth characteristics exhibited by main stems and leaves such as nodes. Therefore, it is difficult to quantify the structure of

crop roots; for example, the partitioning of basic units is challenging. Three dimensional visualizations are an important aspect of studying and recognizing the morphological and structural traits of crop roots. The 3D modeling and visualization methods for root system architecture include 3D static modeling and dynamic growth simulation. The 3D static modeling of root system architecture includes two types of methods: 3D modeling based on simulation algorithms and 3D reconstruction based on in situ detection.

Because it is difficult to obtain the 3D morphological information of crop roots intuitively, the 3D morphological models of crop roots are mainly built using simulation algorithms. In other words, computer graphics simulation algorithms are adapted to conduct 3D modeling and visualization of crop root system by analyzing the morphological structure characteristics of crop roots or are based on statistical analyses of destructive detection data of crop roots. The 3D models of crop root systems constructed by this method have morphological similarity with real root systems.

The associate editor coordinating the review of this manuscript and approving it for publication was Kun Mean Hou .

The first descriptive 3D root system models were presented by Pagès *et al.* [30] and Diggle [8]. Dusserre *et al.* [10] proposed a simple generic model to estimate upland rice root length density from root intersections based on the soil profile. Ge *et al.* [15] established a 3D visual simulation model by using the architectural parameters of the root systems of upland rice. Clark [6] introduced a novel 3D imaging software platform for the high-throughput phenotyping of 3D root traits during seedling development. Pagès *et al.* [31] proposed the Root Typ model and the ArchiSimple model [32] to simplify the simulation algorithm of root spatial distribution as much as possible and further improve the efficiency of root modeling. Zheng and Fang [43] constructed a morphological structure model of rice roots using a combination of dual-scale automaton and L-system modeling. Han and Kuo [16] constructed 3D images of rice roots and quantified phenotypic traits from the images. 3D reconstruction based on in situ detection has been studied intensively in recent years, using techniques such as X-ray computed tomography (XCT) [9], [14], [42], [26], nuclear magnetic resonance imaging (MRI) [34]–[36], neutron radiography (NR) [3], [25], [29], and so on. Mooney *et al.* [27] reviewed the recent research on three-dimensional root reconstruction based on CT images. Zhou *et al.* [45] proposed a three-dimensional visualization and nondestructive detection technique using XCT based on a flat panel detector. Based on root dynamic growth characteristics and their development processes, many researchers have constructed 3D modeling dynamic growth simulations of crop root systems while conducting research into visual simulations of crop root growth processes. Menon *et al.* [24] used data acquired from NR irradiation of a special culture medium to simulate the dynamic growth process of crop root systems. French *et al.* [13] simulated dynamic growth processes by tracking the growth process of Arabidopsis seed roots on agarose plates to obtain data. Yazdanbakhsh and Fisahn [39] used the PlaRoM platform to obtain high-resolution images of crop roots undergoing continuous growth. Jacques *et al.* [18] simulated root growth by creating manual drawings via destructive sampling and hydroponic observations. Leitner *et al.* [20] and [21] established a growth model for plant roots by defining growth rules based on the L-system. Dupuy *et al.* [11] constructed a density distribution function to describe root distribution and combined it with cross-environment feedback to build a root growth model. Bonneu *et al.* [4] integrated root structure information with growth information and constructed a plant root growth model by establishing a convection-diffusion-reaction differential equation. Yang *et al.* [40] and [41] constructed mathematical models of rice root morphological development using crop simulation technologies by analyzing the change patterns of rice root growth during development based on the rice root growth development rule.

The studies described above provided insight into the morphology and physiological functions of rice roots, the relationships between the underground and aboveground parts of

roots, and the effects of cultivation and management practices on roots. However, they did not consider combinations of morphological structures and model parameters. In addition, the image simulation results were not particularly satisfactory, and a systematic operating platform for human-machine interface has not yet been developed. To effectively observe and analyze the growth and distribution characteristics of rice roots in the underground space, this study adopts a “root box” approach, performs experiments, and utilizes specialized morphological analysis software to determine the correlations among rice root morphological parameters such as total root length, total root area and root volume. In this paper, an optimal regression model of the morphological indices of rice roots is fitted by analyzing the mutable characteristics of root morphological indices. A visual simulation of rice root growth is then implemented in a Visual C++ environment with the OpenGL standard graphics library by combining the cubic growth function and B-spline curve methods with L-system modeling to simulate the curves of rice roots, with root nodes as the center. This approach provides a close visual reproduction of the dynamic and continuous growth processes of real root systems under different rice varieties and nitrogen levels.

## II. MATERIALS AND METHODS

### A. EXPERIMENTAL DESIGN

The root box was adopted for the experiments conducted at the experimental station of Jiangxi Agriculture University from 2016 to 2018. In this study, three tested rice cultivars which are popular in Jiangxi province were used for the root box planting experiment. The maximum depth of the rice roots is 28 cm for normal paddy rice and 35 cm for aerobic rice. The length, width and height of each box were 40 cm. Each box was divided into a grid with 16 cells per side, using stainless steel wire mesh. The volume of each cell was 1000 cm<sup>3</sup>. A stainless steel net (with a diameter of 5  $\mu$ m) through which the rice roots can pass freely, was inserted into a 10-cm soil layer in the root box, which serves to cover the rice roots and fix them when they are washed to ensure the integrity of the root, as shown in Fig. 1. The soil in the root box is obtained from paddy soil under no tillage as follows. First, the soil blocks are cut in layers in the paddy field, and then carefully placed into the root box.

The root box with soil is placed into the field 1 to 2 days before the rice is transplanted, and 1 seedling is carefully planted in the center of each root box. The rice seedlings are cultivated using floating seedlings [33]. Then, field management is conducted using the method used in the field test plot where the root box is located.

Two kinds of experiments were conducted for rice with similar growth potential [38]. (1) Tests of rice varieties. Rice varieties of three different plant types (Ganxin 203, Zhongjiazao 17, Luliangyou 35) are adopted as the test materials. (2) Test of nitrogen level. Ganxin 203, a hybrid rice variety, was adopted as the test material, and nutrients were controlled by different amounts of nitrogen fertilizer. The concentration

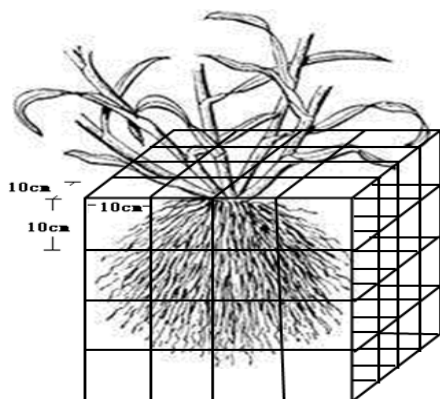


FIGURE 1. Schematic of the root box.

of total nitrogen in normal nutrient solution is 40 mg/L. The experiment was divided into three nitrogen concentration treatment levels: 20 mg/L, 40 mg/L and 80 mg/L. To obtain rice root samples with different nitrogen contents, the above treatments were repeated three times. Other management measures were conducted according to routine practices.

#### B. SAMPLE MEASUREMENT AND DATA PROCESSING

To speed up the cleaning speed and improve the quality, we soaked the roots in NaCl solution to reduce the soil potential and dissociate the charged glue ions. This approach achieved the purpose of loosening the soil and dissolving clay particles. Before collecting the rice roots, the root box was fully immersed in a 100 g/L NaCl solution. Three hours later, it was washed with tap water from top to bottom to obtain complete rice roots. Then, the rice root soil was carefully removed layer by layer. After the rice roots were fully exposed, their morphological characteristics and the occurrences of branching roots could be observed and analyzed. MicroScribe G2 3D digitizer was used to measure adventitious roots, branching roots at different levels and their 3D coordinates. Taking the intersection of the rice root and the ground as the coordinate origin ( $x = 0, y = 0, z = 0$ ), north and east formed the  $y$  and  $x$  positive axes, and vertical direction was adopted as the  $z$  positive axis. The rice roots were measured from the upper section of the root individually. After completing the coordinate measurements of a root, the root was cut and marked using the layering provided by t stainless steel grid. Each layer of roots was scanned using WinRizo root analysis software; then, parameters such as the total root length, total root area and total root volume were measured. After the scanning process was complete, the length of each root in each layer was measured. Subsequently, the roots were dried at  $105^\circ$  for 30 minutes to a constant weight at  $80^\circ$  and weighed with a 1/10,000 analytical balance. Based on the morphological data, the visual simulation of the rice roots was implemented by combining B-spline curve methods with L-system modeling and then using an L-system model to generate self-similar grammatical rules for the fractal reconstruction of rice roots.

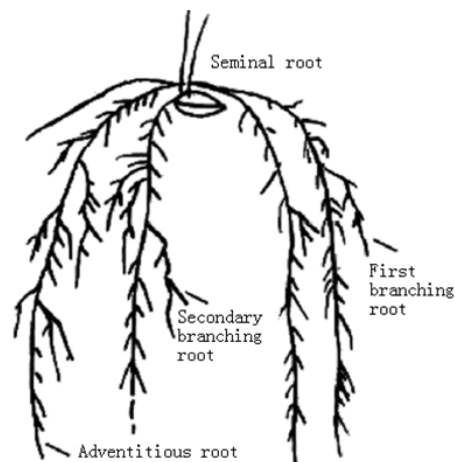


FIGURE 2. Rice root architecture.

### III. PARAMETER SELECTIONS FOR THE RICE ROOT MODEL

#### A. MORPHOLOGICAL CHARACTERISTICS OF RICE ROOTS

Rice roots are fibrous tissues that can be divided into two types: seminal roots and adventitious roots [1]. The seminal root emerges first, followed by the adventitious roots [23]. Only one seminal root occurs during rice seedling growth and development to absorb water and nutrients. Most of the roots are adventitious roots, which are produced from the residual parts of rice stems. The branch roots produced from directly from adventitious roots are called primary branch roots, while those produced from the primary branch roots are called secondary branch roots. Rice branch roots can be generated five to six times under high-yield conditions and their morphological structure exhibits self-similarity. During rice growth and development, the number of adventitious roots changes. During the seedling stage, the number of adventitious roots is small; however, as growth and development continues, the number of adventitious roots increases daily. The number of roots peaks near the heading stage, and the branch roots of all levels intersect. At this time, a dense, strong root structure has formed. An illustration of rice roots is shown in Fig. 2.

#### B. DETERMINING THE INITIAL LOCATION OF THE ROOT NODE

During the process of rice root growth, the initial position of the root node ( $x_0, y_0, z_0$ ) is set; first, the seed root grows vertically downward. According to the geometric space vector and the 3D coordinate operation criterion, the initial position ( $x_i, y_i, z_i$ ) of the root node  $i$  of the branch root is calculated as shown in Formula (1):

$$(x_i, y_i, z_i) = (1 - \text{rnd}(1)) \times (x_{i-1}, y_{i-1}, z_{i-1}) + \text{rnd}(1) \times (x_{i+1}, y_{i+1}, z_{i+1}) \quad (1)$$

where  $\text{rnd}(1)$  represents a random function within the range (0,1).

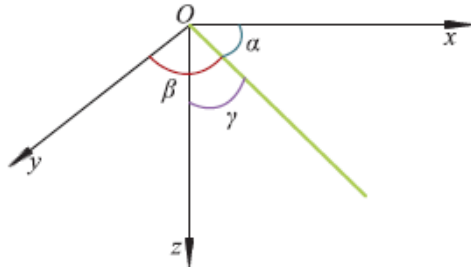


FIGURE 3. Root node growth directions.

C. DETERMINING THE GROWTH DIRECTION OF THE ROOT NODE

The branching roots of rice roots have self-similar topological structures, and their growth directions includes  $\alpha$ ,  $\beta$ ,  $\gamma$ , as shown in Fig. 3. The initial growth direction of branching roots is determined by both the growth direction of their superior roots and by random factors. According to the experimental data, the branching roots are evenly distributed in the horizontal direction  $\alpha$  and randomly in the vertical direction  $\gamma$ . The primary and secondary branching roots have different characteristics.

The root node growth directions ( $D_i$ ) are expressed by Formula (2):

$$D_i = D_{i-1} + (0, \lambda_i, 0) + \zeta_i$$

$$D_{i-1} = (x_{i-1} \times \cos(\alpha_{i-1}), y_{i-1} \times \cos(\beta_{i-1}), z_{i-1} \times \cos(\gamma_{i-1}))$$

(2)

where the growth direction of the superior roots is expressed by  $D_{i-1}$ , which is a vector that points toward the center of the earth for  $(0, \lambda_i, 0)$  which represents the growth direction along which the root node continues to grow downward. The parameter  $\lambda_i$  represents an adjustment factor for the growth of the root node toward the ground. Random deflections of the root node in the vertical direction are adjusted over time by the influence factors.

Primary branching roots and secondary branching roots have different growth characteristics. The statistical range of primary branching roots in the direction is divided into seven different angles, each of which has its own rooting probability. Statistics show that the rooting probability of roots is higher when the value of  $\gamma$  is between  $0^\circ$  and  $90^\circ$  coupled with a smaller rooting probability of other angles, as shown in Table 1. The experimental data show that the values of secondary branching roots are randomly selected within a range between  $30^\circ$  and  $60^\circ$ .

D. SELECTION AND IMPROVEMENT OF THE GROWTH FUNCTION

The growth function of rice roots describes growth factors (such as the length of seminal roots and the number of branch roots produced by adventitious roots) over time during natural growth. The growth function unifies its parameters in the form of expressions, which are obtained by the functional expression of experimental data subjected to statistical analysis. These data are typically obtained directly from rice roots during growth and development. There is a pronounced

TABLE 1. Performance statistics of  $\gamma$  and rooting probability.

$\gamma$	Rooting Probability
$0^\circ \sim 15^\circ$	0.069%
$15^\circ \sim 30^\circ$	0.121%
$30^\circ \sim 45^\circ$	0.221%
$45^\circ \sim 60^\circ$	0.291%
$60^\circ \sim 75^\circ$	0.156%
$75^\circ \sim 90^\circ$	0.098%
$>90^\circ$	0.044%

self-similarity between the main roots and branching roots according to the growth rhythms of rice roots. Thus, in this paper, the cubic growth function is chosen to describe the changes in root growth, as expressed in Formula (3):

$$\frac{dx}{dt} = 6 \frac{\Delta x}{T^2} \left(1 - \frac{t}{T}\right)t$$

(3)

where the parameter T represents a growth cycle and  $t$  represents the time between 0 and T. Root growth increase continuously from the initial value  $x_0$  to the terminal value  $x_{max}$ , and these values are used to describe the cubic equation of the change process and satisfy  $x'(0) = x'(T) = 0$  and  $\Delta x = x_{max} - x_0$ .

However, the growth rates of different roots vary even during the same period and for the same plant, which conflicts with the natural law when the same growth function is used. To overcome this problem, the parameter  $rnd(1)$  is added to the cubic growth function to regulate and control the growth rate. The function definition domain is defined as the growth cycle of its geometric parameters, which is a simple and intuitive approach. The improved growth function not only maintains the growth characteristics of rice roots but also regulates and controls their growth rates using the simple parameter  $rnd(1)$  to solve the problem of growth rate variations among roots. The improved form of this function is shown in Formula (4):

$$\frac{dx}{dt} = \begin{cases} 6rnd(1) \frac{x_{max} - x_{min}}{T^2} \left(1 - \frac{t}{T}\right)t & T_1 \leq t \leq T_2 \\ 0 & t \geq T_2 \end{cases}$$

(4)

where the parameters  $x_{max}$  and  $x_{min}$  represents the maximum and minimum values of the geometric parameters for root growth, respectively. The growth cycle T equals  $T_2 - T_1$ . The parameter  $rnd(1)$  controls the speed of growth, and its range is [0, 1].

Unlike the original growth function, the definition domain of the improved function is the growth cycle, making the expression more intuitive. More importantly, the differences in the growth rates among roots are made more consistent with those of natural growth by including the  $rnd(1)$  value.

IV. CONSTRUCTION AND VERIFICATION OF THE MODEL  
A. DESIGN OF AN L-SYSTEM MODEL BASED ON B-SPLINE CURVES

L-systems use grammars that contain a set of production rules. L-systems allow the user to model complex objects by

successively replacing parts of a simple object [5]. According to the growth characteristics of rice roots, the self-similar topological structures of rice roots can be described using the L-system model generation rules. This paper implements a virtual visual simulation of roots by adopting a fractal reconstruction of the morphological structure of rice roots. B-spline curves are introduced to improve the expression of the L-system model. B-spline curves offer smoothness, convexity and controllability that are beneficial for expressing the curved shapes of rice roots. To gain more local control and allow more complexity in the occluded curves (Zhao 2013), the B-spline curves express the root curve mainly by using start nodes, end nodes, control nodes and de Boor-box recursive formulas. In this study, for the L-system of rice roots, the coordinates of the start nodes and end nodes, which represent the character F between the root segments, are calculated. Then, control nodes are determined. Control nodes can be added between the start nodes and the end nodes or set according to the convex hull direction and the growth space direction of the rice roots. Finally, the curve characteristics of the rice roots are simulated by the de Boor-Cox recursive formulas. The L-system designed based on B-spline curves is shown in Formula (5).

$$\begin{aligned}
 &\omega : X(0, 1) \\
 &p1 : A(i, t) \rightarrow X(i, t) : \pi 1 \\
 &p2 : A(i, t) \rightarrow R(i, t) : \pi 2 \\
 &p3 : X(i, t) : t \neq \alpha T_1 \rightarrow P(i + 1, l_{i+1})X(i + 1, t + 1) \\
 &p4 : X(i, t) : t = \alpha T_1 \rightarrow [P(1, l_1)A(0, 1)]X(i + 1, t + 1) \\
 &p5 : R(i, t) : t \neq \alpha T_2 \rightarrow P(i + 1, l_{i+1})R(i + 1, t + 1) \\
 &p6 : R(i, t) : t = \alpha T_2 \rightarrow [P(1, l_1)A(0, 1)]R(i + 1, t + 1) \\
 &p7 \begin{cases} P(l, l_a) \rightarrow P(j, k - 1, t) \\ P(j, k - 1, t) : k = 1 \rightarrow P(l, l_a) \\ P(j, k - 1, t) : k \neq 1 \rightarrow P(i, k - 2, t) \\ P(i - 1, k - 2, t) \end{cases} \quad (5)
 \end{aligned}$$

where the parameter  $\omega$  represents the initial axiom,  $X(0, 1)$  denotes the initial string that expresses the initial axiom. The growth nodes of roots and the growth parameter of the nodes are represented by  $p$  and  $i$ , respectively. The parameter  $\alpha$  reflects the growth direction of the roots. The growth time interval of the branch roots is represented by the  $t$ . The probabilistic values which the system calls in production formulas  $p1$  and  $p2$  are  $\pi 1$  and  $\pi 2$ , respectively.  $A(i, t)$  represents the growth of branch roots with the probabilities  $\pi 1$  and  $\pi 2$ . The parameter  $l$  represents the length of the branch roots described in the growth function. The start node  $P(0)$  and the end node  $P(n)$  are used to express a curved branch root, and  $n-1$  control node vectors are added between the start nodes and the end nodes based on the root convex hull direction. The initial position  $P(1, l_1)$  is determined by the production formula  $p3$ . The roots produce primary branching roots and secondary branching roots after the growth time interval  $t$ .  $X(i, t)$  and  $R(i, t)$  represent different growth points, and their growth processes are represented by the probabilities  $\pi 1$  and

$\pi 2$  of  $A(i, t)$ . The production formula  $p1$  represents the root rules, and  $P(t)$  represents the root curve. The parameter  $k$  represents the order of B-splines, and the range of parameter  $i$  is  $0 \leq i \leq n$ . The production formulas  $p2$  and  $p3$  are calculated according to the de Boor-Cox recursive formulawhen  $i = j$ ,  $p2$  is called, and when  $i = j - k + r + 1$ ,  $p3$  is called. The parameter  $r$  controls the number of reversals in the B-spline curve. $p7$  is combined with the recursive calculation of the B-spline curves, namely, formula (6). To express the curvature degree of rice roots (Formula (7)) and B-spline curves are used as follows:

$$P_i^{[r]}(t) = \begin{cases} P_i & r = 0 \\ \frac{t - t_i}{t_{i+k-r} - t_i} P_i^{[r-1]}(t) \\ + \frac{t_{i+k-r} - t}{t_{i+k-r} - t_i} P_{i-1}^{[r-1]}(t) & r = 1, 2, \dots, k - 1 \end{cases} \quad (6)$$

$$E_{t,l} = F\{f(h, l) < x\} = \frac{\sum_{i=1}^n f_i(h, l)}{n}, \quad x \in R \quad (7)$$

where  $h$  and  $l$  are quantification parameters and the  $x$  is the degree of the maximal curve.  $E$  and  $F$  represent the curved and linear lines, respectively, between two growth points.

### B. MODEL-CHECKING METHODS

To assess the level of agreement between the model-predicted and the field-observed data [17], the correlation coefficient and variation coefficient analyses are combined. This step is performed to test the accuracy of the rice root model.

1) The correlation coefficient is calculated as follows:

$$r = \frac{\sum_{i=1}^n (x_i - \bar{x})(y_i - \bar{y})}{\sqrt{\sum_{i=1}^n (x_i - \bar{x})^2 \times \sum_{i=1}^n (y_i - \bar{y})^2}} \quad (8)$$

In Formula (8), the parameter  $r$  is the correlation coefficient of the model. The parameters  $i$  and  $x_i$  represent indexes of the samples and the measured values, respectively. The parameter  $\bar{x}$  is the average of the measured values. The parameters  $y_i$  and  $\bar{y}$  are the simulation value and the average simulation value, respectively, and  $n$  represents the number of samples.

$$\alpha \geq \frac{\sum_{i=1}^n (y_i - x_i)^2}{(\bar{x})^2} \quad (9)$$

$$b = \sqrt{\frac{\alpha}{n}} \times \bar{x} \quad (10)$$

In formulas (9) and (10), the parameter  $\alpha$  represents the confidence level of the model, and the band domain between  $y = \bar{x} - b$  and  $y = \bar{x} + b$  represents the confidence band of  $\alpha$ .

2) The variation coefficient is calculated as follows:

$$CV = \frac{SD}{AV} \times 100 \quad (11)$$

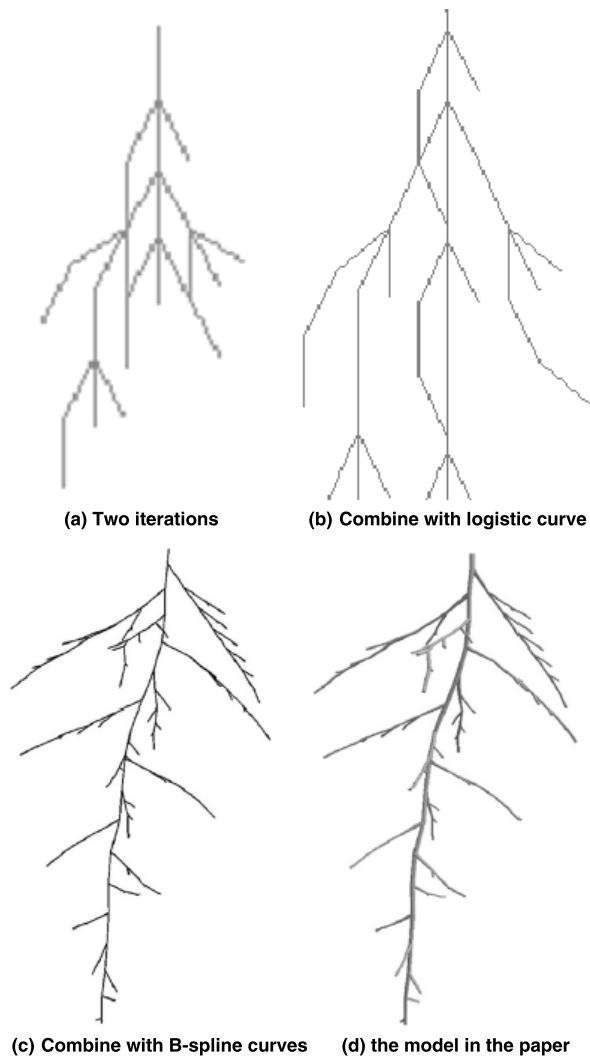


**FIGURE 4.** Schematics of the morphology simulation of individual rice roots.

where  $CV$  is the variation coefficient of the model,  $AV$  is the average value, and  $SD$  is the standard deviation.

## V. RESULTS AND DISCUSSION

### A. CHECKING THE ROOT LENGTH AT DIFFERENT SOIL DEPTHS

At the experimental station of Jiangxi Agriculture University, three tested rice cultivars were used as experimental materials to check the applicability and accuracy of the model. Beginning on March 23, 2018, before tillering, the total root length, root diameter, total root surface area and total root volume of the rice plants were measured once every two days. When the number of roots reached a value from 60 to 100, the plants were measured twice per week; subsequently, they were measured once per week. Three plants of each leaf age before the 10th leaf age were collected, and two plants were collected at each leaf age thereafter. As input parameters this model was calibrated with soil depth data from 10 cm, 20 cm and 30 cm. The test results for the correlation coefficient, confidence degree, confidence band and variation coefficient

**TABLE 2.** Consistency check between simulated and measured root lengths at different soil depths.

Soil depth	$r$	$\alpha$	$y=x \pm b$	$CV$
0~10	0.9895	0.0147	$y=x \pm 0.0366$	5.5466
0~20	0.9886	0.0289	$y=x \pm 0.0331$	7.3271
0~30	0.9723	0.0369	$y=x \pm 0.0454$	10.0025

**TABLE 3.** Consistency check of total root length, root surface area and root volume.

Morphological parameter	Range	Average value	$CV$
Total root length (cm)	113.35~2198.22	667.61	7.6254
Total root area (cm <sup>2</sup> )	14.09~145.14	57.11	7.7368
Total root volume (cm <sup>3</sup> )	0.13~0.98	0.43	7.9547

of the root lengths are shown in Table 2. From the table, we can see that the correlation coefficients between the simulated and measured values in different soil layers are all above 0.9 while the confidence values are all less than 0.04, which is extremely significant. The variation coefficients of the root lengths in the 20 to 30 cm soil layers are above 10, while the variation coefficients of the root lengths in soils from 0 to 20 cm are all below 8. These results indicate that the simulation values are in good agreement with the measured values, demonstrating that the model is effective at simulating the root lengths of rice plants in different soil layers.

### B. CHECKING TOTAL ROOT LENGTH, ROOT SURFACE AREA AND ROOT VOLUME

To further demonstrate the universality of the model, 10 data processed in 2018 were randomly selected to build the model. The total root length, root surface area and root volume of a single rice plant were counted. The test results of varied amplitude, mean value and coefficient of variation are shown in Table 3. As the table shows, the coefficients of variation of total root length, root surface area and root volume do not reach 8, and the coefficients of variation are smaller than the data. The coefficients show a trend in which total root length > total root area > total root volume, indicating good consistency between the measured and simulated values. Root morphology is an important characteristic that varies among rice varieties. The greater the coefficient of variation is [7], the greater the differences are among rice varieties. The coefficient of variation exhibited the following order, as shown in Table 3: total root length > total root area > total root volume.

### C. COMPARISON OF DIFFERENT SIMULATION SOLUTIONS

Using the measured data and the growth trace of the rice root morphological index, the simulation of individual rice

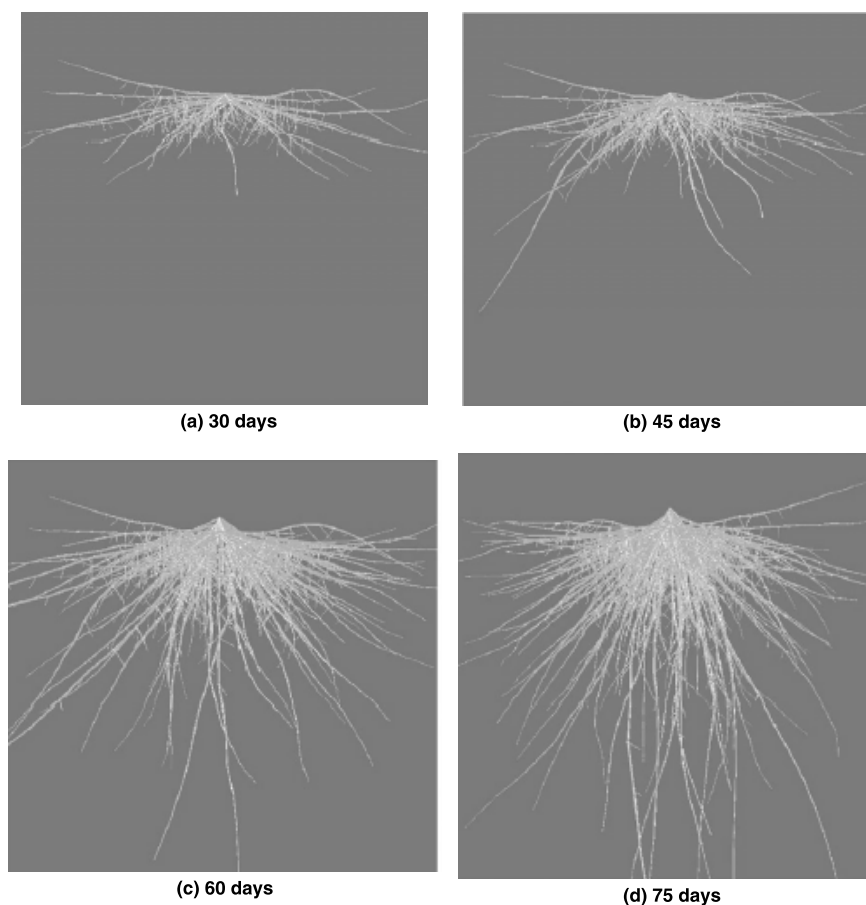


**FIGURE 5.** Diagrams of the dynamic model of rice roots (Ganxin 203).

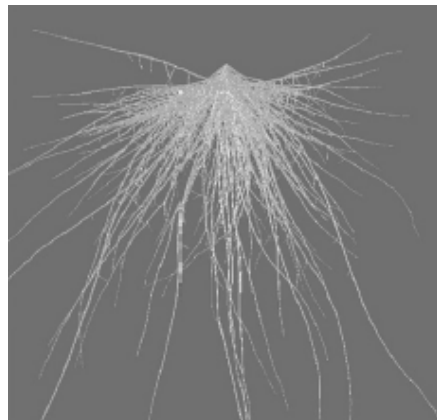
roots in 3D space is performed using four different simulation solutions. The results are shown in Fig. 4.

References [21] and [22] used L-Systems to describe the growth of root systems. Fig. 4(a) depicts the rice root simulation results generated by two iterations of the L-system model. The figure shows that the approach is not ideal with respect to curve degree: the main root and branch roots are overly straight, and the lengths of the branching roots of different levels are the same when generated by L-system iteration. Moreover, the surfaces of the roots are wrinkled and are barely suitable for expressing the topological structures of the rice roots. Using Montefusco's logistic equation [28], the growth parameters and time parameters in the logistic curve equation can be integrated into the L-system. By combining the advantages of the parameterized L-system with the random L-system and using an iterative growth conducted using the growth node as the center, a morphological structure diagram of the rice root system can be obtained, as shown in Fig. 4 (b). The figure shows that the internode root length differs after each iteration; however, the change in the growth amount corresponding to the growth function still fails to conform to the natural growth characteristics of root system. In contrast, based on Pagès' study [32], Fig. 4(c) shows the rice root simulation generated by the improved L-system.

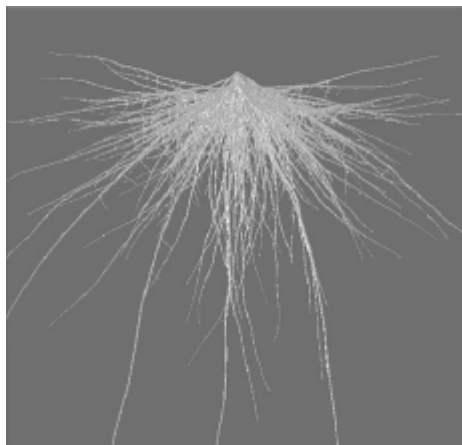
The system is combined with B-spline curves to optimize the 3D display of root images. The results show that the root generation is smoother and that both straight and curved roots are simulated. This simulation expresses the curvature of rice roots and matches natural root morphology more closely than do the simulations in Fig. 4(a) and (b); however, this approach is not effective for performing a 3D generation of the entire root. Therefore, based on the rice root growth traces, terraces are adopted for drawing the root segments, and all the root segments are connected to form a complete root, completing the generation of the rice root simulation shown in Fig. 4(d). As shown in Fig. 4(d), the simulation achieves levels of smoothness and convexity that better reflect the natural smoothness and improves the overall fidelity to real rice roots.

#### D. 3D VISUALIZATION SIMULATION OF RICE ROOTS

Based on the 3D visualization model of single-root rice roots, the rice root model based on morphological parameters and the topological structure of rice roots, 3D visualization simulation of rice roots is performed using the Visual C++ programming language and the OpenGL standard graphics library. In this system, the angles between roots, the curvature degree of branch roots and the extent of root growth are



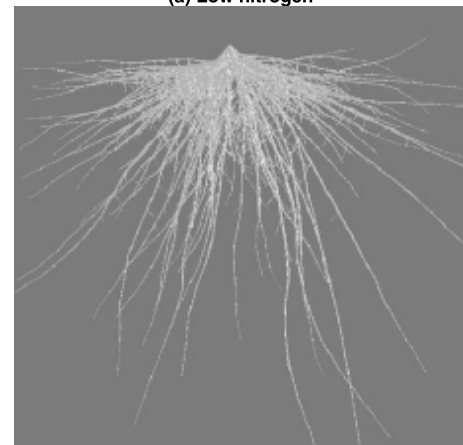
(a) Zhongjiazao 17



(b) Luliangyou 35



(a) Low nitrogen



(b) Hight nitrogen

**FIGURE 6.** Three-dimensional visualization of rice root with different rice.

considered. The system adopts random functions to represent random changes in the various quantities possible and to control the growth of rice roots by controlling the diameter, length and number of iterations of root nodes. The number of iterations is mainly used to control the topological structure of the roots. A larger number of iterations results in denser rice roots. Increases in root diameter and length cause the roots to grow continuously, producing the root growth effect. In this paper, three tested rice cultivars, i.e., Ganxin 203, Zhongjiazao 17 and Luliangyou 35 were used as test materials. According to the descriptions of the morphology and growth characteristics of rice root growth at different development stages, the L-system production formula of root characteristics is expressed by combining the cubic growth function with B-spline curves. The 3D image of rice roots is processed in real time by color rendering, illumination processing and texture mapping. The dynamic growth process of rice roots is illustrated in Fig. 5. Based on the above three-dimensional visual growth system of rice roots, the three-dimensional morphology of rice roots under different varieties and nitrogen treatments was simulated. Fig. 6 shows the simulated root growth for the varieties Zhongjiazao 17 and Luliangyou 35 on day 60. Fig. 7 shows the three-dimensional morphology of

**FIGURE 7.** Three-dimensional visualization of rice root under different nitrogen rate (Ganxin 203).

Ganxin 203 roots under different nitrogen treatments. The visual output of the system is realistic and results in accurately simulated three-dimensional visualization of rice root growth process for different varieties under different nitrogen levels.

In 2018, experimental data were collected for 50 groups. Here, the data from 25 groups were used to build the rice root model, and the data from the other groups were used to test the model. To assess the accuracy of the morphological size of rice roots obtained using the root model, the average values of 25 simulations were computed and compared with the experimental rice root data collected in 2017. The measured and simulated values of total root length, total root area, and total root volume of individual plants were compared. The comparison results are shown in Fig. 8. Statistical analysis results show that the average simulated fitness of the system regarding total root length, surface area and volume reaches 94.82%, 93.86% and 91.96%, respectively. The maximum error between the simulated values and measured values is 3.84%; the minimum error is 0.68%; and the average error value is 1.12%. These findings indicate that the rice root model is able to effectively predict dynamic changes in root



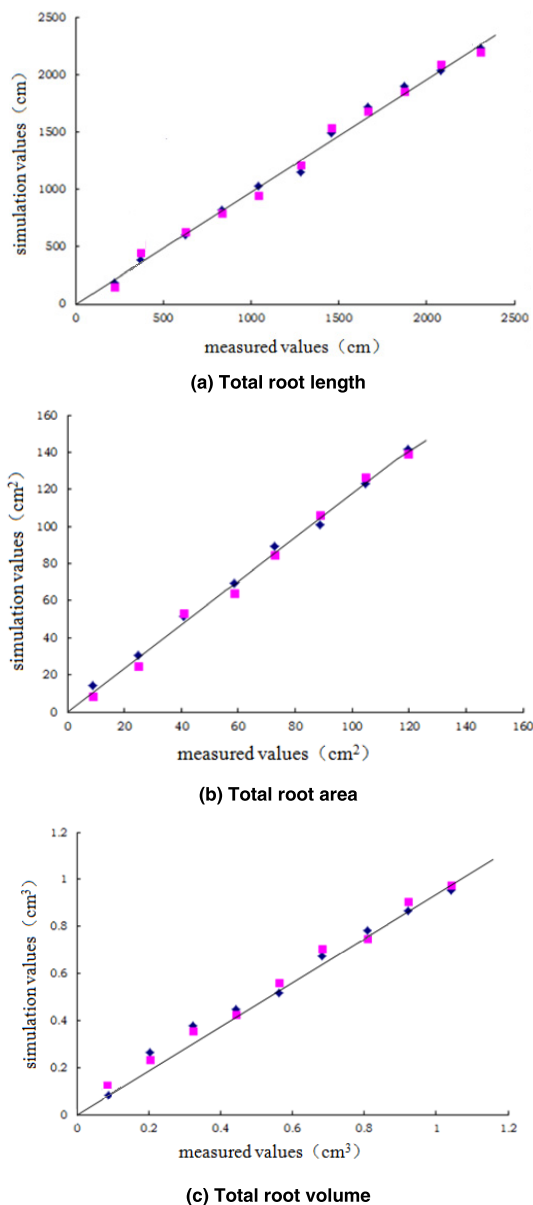


FIGURE 8. Relationships between observed and simulated values.

length, root area and root volume for rice varieties grown under different conditions. The test results show that the root model achieves good reliability.

## VI. CONCLUSION

Accurate model and visual simulation of rice roots are important methods for constructing virtual rice. This paper used a root box experiment to observe and analyze the spatial, morphological, and distributional characteristics of rice roots during their growth and development. An L-system of rice roots was designed in this study and presented in this paper, and a rice root model based on morphological parameters was constructed by optimizing the cubic growth function and using B-spline curves. In addition, a visual simulation of rice roots was implemented using computer graphics technology. The results show that the model accurately simulates the

geometric morphological parameters to show root growth and reveal the development law. The data generated by the model correspond well with the measured data. The correlation coefficient is 0.997, which is very high, and the coefficient of variation is low. The 3D images of the root system show morphological structures that are highly similar to those of actual rice roots, indicating that the root model effectively simulates the growth and development of rice roots. However, this study ignores environmental factors such as air, water, potassium and light conditions. Moreover, sampling error during the collection of the experimental rice root data and other limitations may cause the experimental data to deviate substantially from plants collected under natural conditions. Therefore, in future work, greenhouses based on the field-bus control system will be used to cultivate rice, and a differential L-system will be used to simulate continuous rice root growth. Moreover, additional physiological and ecological factors will be considered in the visual simulation to improve the similarity between simulated images and natural images.

## REFERENCES

- [1] A. Dievert, Y. Coudert, P. Gantet, G. Pauluzzi, J. Puig, D. Fanchon, N. Ahmadi, B. Courtois, E. Guiderdoni, and C. Périn, "Dissecting the biological bases of traits of interest in rice: Architecture and development of the root system," *Cahiers Agricult.*, vol. 22, no. 5, pp. 475–483, Sep. 2013.
- [2] S. L. Atulba, J. Gutierrez, G. W. Kim, S. Y. Kim, M. I. Khan, Y. B. Lee, and P. J. Kim, "Evaluation of rice root oxidizing potential using digital image analysis," *J. Korean Soc. Appl. Biol. Chem.*, vol. 58, no. 3, pp. 463–471, Jun. 2015.
- [3] M. A. Ahmed, M. Zarebanadkouki, A. Kaestner, and A. Carminati, "Measurements of water uptake of maize roots: The key function of lateral roots," *Plant Soil*, vol. 398, nos. 1–2, pp. 59–77, Jan. 2016.
- [4] A. Bonneau, Y. Dumont, H. Rey, C. Jourdan, and T. Fourcaud, "A minimal continuous model for simulating growth and development of plant root systems," *Plant Soil*, vol. 354, nos. 1–2, pp. 211–227, May 2012.
- [5] E. Bohl, O. Terraz, and D. Ghazanfarpour, "Modeling fruits and their internal structure using parametric 3Gmap L-systems," *Vis. Comput.*, vol. 31, no. 6, pp. 819–829, 2015.
- [6] R. T. Clark, R. B. MacCurdy, J. K. Jung, J. E. Shaff, S. R. McCouch, D. J. Aneshansley, and L. V. Kochian, "3-dimensional root phenotyping with a novel imaging and software platform," *Plant Physiol.*, vol. 156, no. 2, pp. 455–465, 2011.
- [7] R. Chittoori, "Root physiological and morphological characteristics of 24 rice varieties selected for diverse grain mineral," *Graellsia*, vol. 69, no. 1, pp. 808–818, 2013.
- [8] A. J. Diggle, "ROOTMAP—A model in three-dimensional coordinates of the growth and structure of fibrous root systems," *Plant Soil*, vol. 105, no. 2, pp. 169–178, Sep. 1988.
- [9] A. Di Iorio, B. Lasserre, and G. S. Scippa, "Root system architecture of quercus pubescens trees growing on different sloping conditions," *Ann. Botany*, vol. 95, no. 2, pp. 351–361, 2005.
- [10] J. Dusserre, A. Audebert, A. Radanielson, and J.-L. Chopart, "Towards a simple generic model for upland rice root length density estimation from root intersections on soil profile," *Plant Soil*, vol. 325, nos. 1–2, pp. 277–288, Dec. 2009.
- [11] L. Dupuy, P. J. Gregory, and A. G. Bengough, "Root growth models: Towards a new generation of continuous approaches," *J. Exp. Botany*, vol. 61, no. 8, pp. 2131–2143, May 2010.
- [12] V. M. Dunbabin, J. A. Postma, and A. Schnepf, "Modelling root-soil interactions using three-dimensional models of root growth, architecture and function," *Plant Soil*, vol. 372, nos. 1–2, pp. 93–124, 2013.
- [13] A. French, S. Ubeda-Tomás, T. J. Holman, M. J. Bennett, and T. Pridmore, "High-throughput quantification of root growth using a novel image-analysis tool," *Plant Physiol.*, vol. 150, no. 4, pp. 1784–1795, 2009.
- [14] R. J. Flavel, C. N. Guppy, M. Tighe, M. Watt, A. McNeill, and I. M. Young, "Non-destructive quantification of cereal roots in soil using high-resolution X-ray tomography," *J. Exp. Botany*, vol. 63, no. 7, pp. 2503–2511, Apr. 2012.

- [15] Y. Ge, Z. Ge, H. Yi, P. Li, and H. Guo, "Visual simulation of upland rice root as related to soil compaction," in *Proc. 2nd Int. Conf. Digit. Manuf. Autom.*, Aug. 2011, pp. 1392–1394.
- [16] T.-H. Han and Y.-F. Kuo, "Developing a system for three-dimensional quantification of root traits of rice seedlings," *Comput. Electron. Agricult.*, vol. 152, pp. 90–100, Sep. 2018.
- [17] C. J. Dash, A. Sarangi, D. K. Singh, A. K. Singh, and P. P. Adhikary, "Prediction of root zone water and nitrogen balance in an irrigated rice field using a simulation model," *Paddy Water Environ.*, vol. 13, no. 3, pp. 281–290, Jul. 2015.
- [18] J. Le Bot, V. Serra, J. Fabre, X. Draye, S. Adamowicz, and L. Pagès, "DART: A software to analyse root system architecture and development from captured images," *Plant Soil*, vol. 326, nos. 1–2, pp. 261–273, Jan. 2010.
- [19] T. Kreszies, L. Schreiber, and K. Ranathunge, "Suberized transport barriers in Arabidopsis, barley and rice roots: From the model plant to crop species," *J. Plant Physiol.*, vol. 227, pp. 75–83, Aug. 2018.
- [20] D. Leitner and A. Schnepf, "Root growth simulation using L-systems," in *Proc. ALGORITHMY*, vol. 2009, 2009, pp. 313–320.
- [21] D. Leitner, S. Klepsch, G. Bodner, and A. Schnepf, "A dynamic root system growth model based on L-Systems: Tropisms and coupling to nutrient uptake from soil," *Plant Soil*, vol. 332, nos. 1–2, pp. 177–192, Jul. 2010.
- [22] D. Leitner, S. Klepsch, A. Knieß, and A. Schnepf, "The algorithmic beauty of plant roots—an L-system model for dynamic root growth simulation," *Math. Comput. Model. Dyn. Syst.*, vol. 16, no. 6, pp. 575–587, Dec. 2010.
- [23] S. Morita and J. Abe, "Modeling root system morphology in rice," in *Biology of Adventitious Root Formation*, vol. 62, no. 1. Boston, MA, USA: Springer, 1994, pp. 191–202.
- [24] M. Menon, B. Robinson, S. E. Oswald, A. Kaestner, K. C. Abbaspour, E. Lehmann, and R. Schulin, "Visualization of root growth in heterogeneously contaminated soil using neutron radiography," *Eur. J. Soil Sci.*, vol. 58, no. 3, pp. 802–810, Jun. 2007.
- [25] A. B. Moradi, H. M. Conesa, B. Robinson, E. Lehmann, G. Kuehne, A. Kaestner, S. Oswald, and R. Schulin, "Neutron radiography as a tool for revealing root development in soil: Capabilities and limitations," *Plant Soil*, vol. 318, nos. 1–2, pp. 243–255, 2009.
- [26] S. Mairhofer, S. Zappala, S. R. Tracy, C. Sturrock, M. Bennett, S. J. Mooney, and T. Pridmore, "RooTrak: Automated recovery of three-dimensional plant root architecture in soil from X-ray microcomputed tomography images using visual tracking," *Plant Physiol.*, vol. 158, no. 2, pp. 561–569, 2012.
- [27] S. J. Mooney, T. P. Pridmore, J. Helliwell, and M. J. Bennett, "Developing X-ray computed tomography to non-invasively image 3-D root systems architecture in soil," *Plant Soil*, vol. 352, nos. 1–2, pp. 1–22, Mar. 2012.
- [28] E. Montefusco, B. Pellacci, and G. Verzini, "Fractional diffusion with Neumann boundary conditions: The logistic equation," *Discrete Continuous Dyn. Syst.-Ser. B (DCDS-B)*, vol. 18, no. 8, pp. 2175–2202, 2013.
- [29] S. E. Oswald, M. Menon, A. Carminati, P. Vontobel, E. Lehmann, and R. Schulin, "Quantitative imaging of infiltration, root growth, and root water uptake via neutron radiography," *Vadose Zone J.*, vol. 7, no. 3, pp. 1035–1047, Aug. 2008.
- [30] L. Pagès, M. O. Jordan, and D. Picard, "A simulation model of the three-dimensional architecture of the maize root system," *Plant Soil*, vol. 119, no. 1, pp. 147–154, Sep. 1989.
- [31] L. Pagès, G. Vercambre, J.-L. Drouet, F. Lecompte, C. Collet, and J. Le Bot, "Root typ: A generic model to depict and analyse the root system architecture," *Plant Soil*, vol. 258, no. 1, pp. 103–119, Jan. 2004.
- [32] L. Pages, D. Moreau, V. Sarlikioti, H. Boukcim, and C. Nguyen, "ArchiSimple: A parsimonious model of the root system architecture," in *Proc. IEEE 4th Int. Symp. Plant Growth Modeling, Simulation, Visualizat. Appl.*, Oct. 2012, pp. 297–303.
- [33] A. P. Punsalan, *The Germination of HELONIAS BULLata L. (Swamppink) in Response to Flooded, Saturated, and Dry Conditions*. Cullowhee, NC, USA: Western Carolina Univ., 2013.
- [34] D. Pflugfelder, R. Metzner, D. Van Dusschoten, R. Reichel, S. Jahnke, and R. Koller, "Non-invasive imaging of plant roots in different soils using magnetic resonance imaging (MRI)," *Plant Methods*, vol. 13, no. 1, pp. 102–111, 2017.
- [35] H. Schulz et al., "Plant root system analysis from MRI images, computer vision, imaging and computer graphics," in *Theory and Application*, vol. 359, no. 1. Berlin, Germany: Springer, 2013, pp. 411–425.
- [36] L. Stingaciu, H. Schulz, A. Pohlmeier, S. Behnke, H. Zilken, M. Javaux, and H. Vereecken, "In situ root system architecture extraction from magnetic resonance imaging for water uptake modeling," *Vadose Zone J.*, vol. 12, no. 1, pp. 1–9, Feb. 2013.
- [37] K. A. T. N. Somaweera, D. N. Sirisena, W. A. J. M. De Costa, and L. D. B. Suriyagoda, "Age-related morphological and physiological responses of irrigated rice to declined soil phosphorus and potassium availability," *Paddy Water Environ.*, vol. 15, no. 3, pp. 499–511, Jul. 2017.
- [38] Q. Xu, L. Tang, D. Gu, H. Jiang, and W. Cao, "Architectural parameter-based three dimensional modeling and visualization of rice roots," *Trans. Chin. Soc. Agricult. Eng.*, vol. 26, no. 10, pp. 188–194, 2010.
- [39] N. Yazdanbakhsh and J. Fisahn, "High throughput phenotyping of root growth dynamics, lateral root formation, root architecture and root hair development enabled by PlaRoM," *Funct. Plant Biol.*, vol. 36, no. 11, p. 938, 2009.
- [40] L. Yang, Q. Qiang Zhou, Y. Wan, and H. Jiao He, "Three dimensional visual simulation of rice root growth," in *Proc. Int. Conf. Multimedia Technol.*, Jul. 2011, pp. 3289–3292.
- [41] L. Yang, J. Peng, and H. Y. Yang, "Three dimensional growth modeling of rice root based on differential L-system," *Trans. Chin. Soc. Agricult. Mach.*, vol. 50, no. 10, pp. 208–214, 2019.
- [42] J. Zhu, P. A. Ingram, P. N. Benfey, and T. Elich, "From lab to field, new approaches to phenotyping root system architecture," *Current Opinion Plant Biol.*, vol. 14, no. 3, pp. 310–317, Jun. 2011.
- [43] Z. Boyin and F. Yao, "Construction and visualization of rice roots model based on artificial life," in *Proc. Int. Conf. Comput. Sci. Netw. Technol.*, Apr. 2012, pp. 539–544.
- [44] J. Zhao and E. Mansfield, "Discrete variational calculus for B-spline curves," *Math. Comput. Sci.*, vol. 7, no. 2, pp. 185–199, Jun. 2013.
- [45] X. Zhou, X. Cao, C. Zhang, H. Yan, Y. Li, and X. Luo, "A method of 3D nondestructive detection for plant root in situ based on CBCT imaging," in *Proc. 7th Int. Conf. Biomed. Eng. Informat.*, Oct. 2014, pp. 110–115.



**LE YANG** received the B.S. degree in computer science and technology from the Chang'an University, Xi an, China, in 2003, and the M.S. degree in computer system architecture from Jiangxi Normal University, Nanchang, China, in 2008. He is currently an Associate Professor with the Jiangxi Agricultural University. He is also a person in charge of a national scientific research project and a provincial scientific research project. He has authored two books and authored or coauthored more than 50 academic articles. His research interests mainly focused on software dormalization, automation, and agricultural information technology.



**JUN PENG** received the B.S. degree in computer science and technology from Jiangxi Normal University, Nanchang, China, in 2001, and the M.S. degree in software engineering from Nanchang University, Nanchang, in 2008. He is currently an Associate Professor with Jiangxi Agricultural University. He has authored three books and authored or coauthored more than 30 academic articles. His research interests mainly focused on agricultural informatization, electronic commerce, and knowledge engineering.



**PENG SHAO** received the M.Sc. degree from the School of Computer and Information Engineering, Jiangxi Agricultural University, China, in 2011, and the Ph.D. degree from the State Key Lab of Software Engineering, Wuhan University, China, in June 2016. He is currently working with the School of Computer and Information Engineering, Jiangxi Agricultural University. His current research interests include artificial intelligence, large-scale optimization, image processing, and related real world applications. He has published more than ten research articles in these fields.